


RESEARCH

Open Access



JAK2 as a surface marker for enrichment of human pluripotent stem cells-derived ventricular cardiomyocytes

Lee Chuen Liew¹, Boon Min Poh¹, Omer An², Beatrice Xuan Ho¹, Christina Ying Yan Lim¹, Jeremy Kah Sheng Pang¹, Leslie Y. Beh¹, Henry He Yang² and Boon-Seng Soh^{1,3*} 

Abstract

Background Human pluripotent stem cell (hPSC)-derived cardiomyocytes (CMs) hold great promise for cardiac disease modelling, drug discovery and regenerative medicine. Despite the advancement in various differentiation protocols, the heterogeneity of the generated population composed of diverse cardiac subtypes poses a significant challenge to their practical applications. Mixed populations of cardiac subtypes can compromise disease modelling and drug discovery, while transplanting them may lead to undesired arrhythmias as they may not integrate and synchronize with the host tissue's contractility. It is therefore crucial to identify cell surface markers that could enable high purity of ventricular CMs for subsequent applications.

Methods By exploiting the fact that immature CMs expressing myosin light chain 2A (MLC2A) will gradually express myosin light chain 2V (MLC2V) protein as they mature towards ventricular fate, we isolated signal regulatory protein alpha (SIRPA)-positive CMs expressing intracellular MLC2A or MLC2V using MARIS (method for analysing RNA following intracellular sorting). Subsequently, RNA sequencing analysis was performed to examine the gene expression profile of MLC2A+ and MLC2V+ sorted CMs. We identified genes that were significantly up-regulated in MLC2V+ samples to be potential surface marker candidates for ventricular specification. To validate these surface markers, we performed immunostaining and western blot analysis to measure MLC2A and MLC2V protein expressions in SIRPA+ CMs that were either positive or negative for the putative surface markers, JAK2 (Janus kinase 2) or CD200. We then characterized the electrophysiological properties of surface marker-sorted CMs, using fluo-4 AM, a green-fluorescent calcium indicator, to measure the cellular calcium transient at the single cell level. For functional validation, we investigated the response of the surface marker-sorted CMs to vernakalant, an atrial-selective anti-arrhythmic agent.

Results In this study, while JAK2 and CD200 were identified as potential surface markers for the purification of ventricular-like CMs, the SIRPA+/JAK2+ population showed a higher percentage of MLC2V-expressing cells (~90%) compared to SIRPA+/CD200+ population (~75%). SIRPA+/JAK2+ sorted CMs exhibited ventricular-like electrophysiological properties, including slower beating rate, slower calcium depolarization and longer calcium repolarization duration. Importantly, vernakalant had limited to no significant effect on the calcium repolarization duration of SIRPA+/JAK2+ population, indicating their enrichment for ventricular-like CMs.

*Correspondence:

Boon-Seng Soh

bssoh@imcbs.a-star.edu.sg

Full list of author information is available at the end of the article



© The Author(s) 2023. **Open Access** This article is licensed under a Creative Commons Attribution 4.0 International License, which permits use, sharing, adaptation, distribution and reproduction in any medium or format, as long as you give appropriate credit to the original author(s) and the source, provide a link to the Creative Commons licence, and indicate if changes were made. The images or other third party material in this article are included in the article's Creative Commons licence, unless indicated otherwise in a credit line to the material. If material is not included in the article's Creative Commons licence and your intended use is not permitted by statutory regulation or exceeds the permitted use, you will need to obtain permission directly from the copyright holder. To view a copy of this licence, visit <http://creativecommons.org/licenses/by/4.0/>. The Creative Commons Public Domain Dedication waiver (<http://creativecommons.org/publicdomain/zero/1.0/>) applies to the data made available in this article, unless otherwise stated in a credit line to the data.

Conclusion Our study lays the groundwork for the identification of cardiac subtype surface markers that allow purification of cardiomyocyte sub-populations. Our findings suggest that JAK2 can be employed as a cell surface marker for enrichment of hPSC-derived ventricular-like CMs.

Keywords Cardiac differentiation, Human pluripotent stem cells, Ventricular cardiomyocytes, Cell surface marker, Cardiac subtypes, JAK2

Introduction

The discovery of human pluripotent stem cells, including human embryonic stem cells (hESCs) and human-induced pluripotent stem cells (hiPSCs) [1, 2], has opened a new avenue for biomedical research, ranging from cell therapy to disease modelling, and drug screening, owing to their plasticity to be able to give rise to almost all of the clinically relevant cell types. Cardiovascular diseases (CVDs), being one of the leading causes of death worldwide, are among the diseases that are extensively studied using hPSCs. Particularly, the generation of many CVD models, both *in vitro* and *in vivo*, has provided useful molecular insights to heart diseases [3–5]. However, hPSCs-derived cardiomyocytes (hPSC-CMs) generated from the current differentiation protocols remain highly heterogeneous, typically giving rise to different cardiac subtypes such as atrial-, ventricular- and pacemaker-like cells [6, 7]. These different subtypes of cardiomyocytes that exhibited different phenotypes, electrophysiological properties and functions [7–9] represent the major challenge for downstream applications of hPSC-CMs. For instance, the use of mixed population of cardiomyocytes in modelling chamber-specific cardiac disease may confound the disease phenotypes and consequently compromise the credibility of the drug response outcome [4], which in turn leads to limited success in drug discovery for region-specific heart diseases. More importantly, transplanting a heterogeneous pool of hPSC-CMs into an infarcted heart might disturb normal electrical impulse propagation in the heart, leading to undesirable therapeutic outcomes, such as arrhythmias [10]. Therefore, the prerequisite for translational applications of hPSC-CMs is to generate and isolate a relatively pure population of cardiomyocyte subtype for subsequent applications.

Over the last few decades, there have been numerous reports on advancements in differentiating cardiomyocyte subtypes. For instance, retinoic acid (RA) has been identified as a crucial factor in specifying atrial cell fate [11, 12], while inhibition of the canonical Wnt pathway with IWR-1 has been shown to promote differentiation towards ventricular cardiomyocytes [13]. Nonetheless, the challenge of obtaining a homogeneous population of cells still persists, as differentiation protocols appear to be cell line-dependent. On top of modulating relevant signalling pathways via small molecules, hPSC line

harbouring fluorescent reporter driven by the transcriptional control of human MYL2 promoter (MLC2V) [14, 15] and chick ovalbumin upstream promoter transcription factor II (COUP-TFII) [16] were also employed to facilitate the isolation of ventricular and atrial cardiomyocytes, respectively. However, the major drawback of such cardiomyocytes is the involvement of virus-mediated gene transfer that has raised safety issues such as unknown off-target mutagenesis or immunogenicity and therefore holding them back from further clinical translation.

To overcome the challenge of cellular heterogeneity without genetic manipulation, we sought to identify novel cell surface markers for live cell sorting of ventricular-specific CMs. Through RNA isolation of SIRPA+CMs that were sorted based on intracellular MLC2A or MLC2V expression using MARIS, we performed RNA sequencing and identified JAK2 as a potential surface marker for purification of ventricular-like cardiomyocytes. We showed that SIRPA+/JAK2+ cell population was enriched for ventricular-like CMs, in both H7 and BJ lines (~90%). These SIRPA+/JAK2+ sorted CMs expressed high level of ventricular-specific marker, MLC2V, validated through immunofluorescent staining and western blot analysis. Additionally, electrophysiological characterization of the SIRPA+/JAK2+ sorted CMs demonstrated properties similar to ventricular CMs, such as prolonged calcium repolarization phase. Importantly, SIRPA+/JAK2+ sorted cardiomyocytes, which are ventricular-like CM, did not respond to vernakalant treatment, an atrial-selective anti-arrhythmic agent. Therefore, our findings suggest that JAK2 can be employed as a cell-surface marker to facilitate the isolation of hPSC-derived ventricular cardiomyocytes from the heterogeneous CMs cultures.

Methods

Pluripotent stem cell lines culture

The human ESC lines, H7 and ES03, and human iPSC line derived from BJ fibroblasts (all cell lines were purchased from WiCell) were cultured on Matrigel (Corning, USA)-coated plates with StemMACS™ iPS-Brew XF medium (Miltenyi Biotec). Culture medium was changed daily, and cells were passaged using ReLeSR (STEMCELL Technologies) after reaching 80–90% confluency.

Cardiomyocyte differentiation, selection and maturation

For cardiomyocyte differentiation, pluripotent stem cells were dissociated into single cells using Accutase (Nacalai-Tesque) and seeded on Matrigel-coated plates in Stem-MACS™ iPS-Brew XF. At 90–95% confluency, cardiac differentiation was induced by modulating Wnt signalling using Gsk-3 (glycogen synthase kinase 3) and Wnt inhibitors, as described by Lian et al., 2013 [17]. At Day 7, the media was replaced with RPMI1640 containing MACS NeuroBrew-21 (Miltenyi Biotec) and refreshed every 2 days. At day 16, PSC-CMs were then cultured in glucose-depleted culture medium supplemented with fatty acid (GFAM) for cardiomyocyte selection and metabolic maturation. The GFAM medium contains RPMI without glucose supplemented with MACS NeuroBrew-21, galactose (10 mM), oleic acid (100 μ M) and palmitate acid (50 μ M) [18].

Isolation of MLC2A+ and MLC2V+ CMs by MARIS

MLC2A+ and MLC2V+ CMs were isolated from PSC-CMs using a modified MARIS method, as previously reported [19, 20]. Briefly, at 3 weeks post-contraction, hPSC-CMs were dissociated into single cells using Accutase. Cells were then fixed and permeated with 4% paraformaldehyde (PFA). Anti-human CD172a/b (SIRP α/β)-PECy7 (1:200; 323,808; Biolegend), anti-MLC2a-FITC (1:10; 130–106–141; Miltenyi Biotec) and anti-MLC2v-PE (1:10; 130–106–133; Miltenyi Biotec) antibodies were diluted in blocking buffer (1% bovine serum albumin (BSA)) and 0.2% saponin (Sigma) in phosphate-buffered saline (PBS) supplemented with 50 U/ml Superase. In (Ambion) and incubated with the cell suspension for 1 h. The cells were then washed with Dulbecco's PBS (DPBS) before FACS on BD FACS Aria. Sorted cells were treated with Proteinase K for 1 h at 50 °C before addition of Trizol LS (Invitrogen) for RNA extraction. DNase treatment using Turbo DNA-free (Ambion) was performed to remove contaminating genomic DNA.

RNA sequencing

Identification of ventricular-specific surface marker

Gene expression profiling has been performed by using CSI NGS Portal [21]. Briefly, raw fastq files were trimmed by Trimmomatic [22] for adapter removal. The clean reads were aligned to the reference human genome (hg19) by using STAR [23] (v2.7.3a) with default parameters. The gene expression quantification was done by using HTSeq-count [24] (v0.11.2) in strand-specific mode “-s reverse” to obtain raw read counts for each gene, and read counts only from the sense strand are used. First, hierarchical clustering was

performed with regionReport [25] to compare the gene expression profiles of the samples, by using the top 500 genes with the highest variance across the samples. Then, the differential gene expression analysis was performed by using DESeq2 [26] (v1.24.0) starting from the raw read counts by comparing BJ MLC2V samples to BJ MLC2A samples after collapsing the samples within each group (2 for BJ MLC2V and 3 for BJ MLC2A samples) as replicates. The genes that are not expressed or lowly expressed (read counts ≤ 2 on average per sample) were removed from the analysis. In total, 1349 and 1516 genes were significantly up- and down-regulated, respectively, in the BJ MLC2V samples compared to BJ MLC2A samples, after correction for multiple hypothesis testing (\log_2 fold change > 1 , $P_{\text{adj}} < 0.05$, using Benjamini–Hochberg method). The same analysis was repeated to for ESO3 MLC2V and BJ MLC2A samples; 1904 and 2811 genes were significantly up- and down-regulated, respectively. Genes that were up-regulated in both sets of comparisons, and were found to encode for surface markers were identified as potential surface marker candidates for ventricular specification. The top 30 genes were then used for heatmap plotting in R.

Gene expression profiling of SIRPA+/JAK2+ sorted CMs, MYL2-TdTomato reporter-derived ventricular CMs, adult human ventricle and atrial samples

RNA extraction from SIRPA+/JAK2+ and MYL2-TdTomato+ sorted CMs was performed using Trizol (Invitrogen), followed by DNase treatment with Turbo DNA-free (Ambion) to eliminate contaminating genomic DNA. RNA-seq data from adult human atrial and ventricular samples were obtained from an existing database (GEO accession: GSE81585). These RNA-seq data were then quality trimmed and filtered using fastp [27, 28] with default settings. RNA-seq reads were then mapped to the GRCh38 reference human genome assembly using STAR [23] with default parameters, using GENCODE v38 annotations. FPKM values were then tabulated using FPKM Count in the RSeQC package [29] and averaged across biological replicates. Raw counts were processed following the vignette of the DESeq2 package [30]. Briefly, raw counts were read using the DESeq2 package and pre-filtered to remove genes that have less than 10 counts across all samples. The human atria and ventricle samples were contrasted to identify the top 100 up-regulated genes in the atria and ventricle, with an adjusted p value < 0.05 and a \log_2 fold change > 1 . Variance stabilizing transformation was used to stabilize the variance across the means of all samples. Gene expression heatmaps were plotted using normalized and scaled gene expression levels across all samples.

Florescence activated cell sorting (FACS)

Cardiomyocyte (at least day 45 of culture) were dissociated using Accutase. Cells were then co-stained with anti-human CD172a/b (SIRP α/β)-conjugated antibody (1:200; 323,808; Biolegend), and either anti-human CD200 FITC-conjugated antibody (1:20; 130-106-015; Miltenyi Biotec), or rabbit-anti-JAK2 unconjugated antibody (1:20; PA511267; Invitrogen) in blocking buffer (1% foetal bovine serum (FBS) in PBS) for 1 h at 37 °C. The secondary antibody used was Alexa Fluor 488-conjugated donkey anti-rabbit (1:1000; Thermo Scientific). Stained cardiomyocytes were washed thoroughly with PBS before the resuspended in FACS buffer (0.5% FBS and 1% BSA in PBS). FACS was performed using BD FACSAria II or BD FACSAria™ Fusion Flow Cytometer (BD Bioscience). Unstained sample was used as control populations.

Immunostaining

Surface marker-sorted cardiomyocytes were seeded on a 96-well plate coated with Matrigel at a density of 100 k cells per well. Two to 3 days after seeding, the cells were fixed with 4% PFA (Nacalai-Tesque, Japan) for 15 min at room temperature (RT) and permeabilized with PBS containing 0.2% Triton X-100 (Promega, USA) for 15 min at RT. The cells were then exposed to blocking buffer consisting of 1% FBS for 1 h at RT. Next, cells were incubated with primary antibodies in blocking buffer for overnight at 4 °C, followed by incubation with appropriate fluorescence-tagged secondary antibodies at RT for 1 h in the dark. The primary antibodies used were rabbit-anti-human MLC2V (1:400; 10,906-1-AP; Proteintech) and mouse-anti-human MLC2A (1:200; 311 011; Synaptic Systems). The secondary antibodies used were Alexa Fluor 594-conjugated donkey anti-rabbit and Alexa Fluor 488-conjugated donkey anti-mouse (1:1000; Thermo Scientific). Nuclei were counterstained with 4',6-diamidino-2-phenylindole (DAPI) (1:1000; AAT Biorequest, USA) at RT for 5 min. Cells were washed thrice in PBS between each step. Stained cells were visualized with Nikon ECLIPSE Ti-S fluorescent microscope and analysed with Nikon's NIS-Elements AR analysis software.

Western blot analysis

Cells were lysed in RIPA buffer (Thermo Scientific, USA) containing cOmplete™ Protease Inhibitor Cocktail (Sigma-Aldrich, USA). Protein concentration was quantitated with Pierce™ BCA Protein Assay Kit (Thermo Scientific, USA) in accordance to manufacturer's recommendations. Protein lysates were resolved in 12% SDS-PAGE gels in Tris-Glycine-SDS buffer and transferred to a nitrocellulose membrane (Bio-Rad, USA) using the Trans-Blot® Turbo™ transfer system (Bio-Rad, USA). Membranes were blocked with 5% blotting-grade

blocker (1,706,404; Bio-Rad) in tris-buffered saline with 0.1% tween20 (TBS-T) for 30 min and subsequently incubated with primary antibodies overnight at 4 °C. The following primary antibodies were used: rabbit-anti-human MLC2V (1:1000; 10,906-1-AP; Proteintech), mouse-anti-human MLC2A (1:1000; 311 011; Synaptic Systems), rabbit-anti-GAPDH (1:1000; D16H11, Cell Signalling Technologies) and mouse-anti-GAPDH (1:1000; ab16048, Abcam). The blots were subsequently incubated with respective HRP-conjugated antibodies at 1:1000 dilution for 1 h at room temperature. Labelled proteins were detected with Clarity™ ECL Western Substrate (Bio-Rad, USA) and visualized with Fujifilm LAS-3000 imaging system (Fujifilm). Densitometry analysis was performed with Image Lab software (Bio-Rad, USA).

Fluorescent imaging of calcium transient

Surface marker-sorted cardiomyocytes were seeded on a 96-well plate coated with Matrigel at a density of 80 k-100 k cells per well. Calcium transient imaging was performed after resumption of cell contraction was observed. Prior to imaging, the cells were washed twice with Tyrode's Salt solution with 1× sodium bicarbonate (Sigma-Aldrich, T2397). The cells were then incubated in Tyrode's Salt solution containing 2.5 μ M of the calcium indicator Fluo-4 AM (ThermoFisher, F14201) with 0.02% Pluronic™ F-127 (ThermoFisher, P3000MP) for 45 min in a 5% CO₂ incubator at 37°C. Fluo-4 AM loading solution was then removed, the cells were washed and subsequently incubated in Tyrode's Salt for another 20 min in the incubator before imaging. Calcium transients of sorted CMs were recorded using Nikon ECLIPSE Ti-S fluorescent microscope for 30 s and video data were analysed using Nikon's NIS-Elements AR. Fluorescent intensity values were processed using our self-compiled code in R (RStudio version 1.2.1335/Base R version 3.6.3) to identify fluorescent peaks corresponding to single cardiac contraction [31].

Vernakalant treatment

Surface marker-sorted cardiomyocytes seeded on 96-well plate (at density of 80-100 k cells per well) were incubated with the calcium indicator Fluo-4 AM loading solution as previously mentioned, and calcium transients imaging was recorded as data for pre-treatment samples. For post-treatment samples, after 45 min of incubation with the Fluo-4 AM loading solution, cells were then treated with 10 μ M of vernakalant hydrochloride (HY-14183; MedChemExpress) in Tyrode's Salt solution for 30 min, followed by calcium transients imaging. For withdrawal samples, vernakalant hydrochloride solution was removed by washing twice with Tyrode's Salt solution before imaging.

Statistical analysis

All the experimental data are presented as mean \pm SD. Statistical differences of the data were determined using an unpaired Student's *t* test. The equality of the variances was tested using an *F* test. All *p* values are two-tailed. A value of *P* < 0.05 was considered statistically significant.

Results

Potential surface markers shortlisted for purification of ventricular-specific cardiomyocytes

It is known that myosin regulatory light chain 2 encoded by MYL7 gene (also referred to as MLC2A) was predominantly expressed in all immature cardiomyocytes. In addition to MLC2A protein, immature CMs will gradually express MLC2V protein (encoded by MYL2 gene) as they mature towards ventricular fate, whereas atrial CMs will continue to express only MLC2A throughout the maturation process [32, 33]. As such, we reasoned that by conducting gene expression profiling on MLC2A- and MLC2V-expressing cardiomyocytes using RNA-seq approach, we could identify novel surface markers that aid in distinguishing ventricular cells from heterogeneous CMs culture.

As shown in Fig. 1A, cardiomyocytes were first differentiated from 2 hPSC lines (BJ and ES03) using published protocol [17]. Induction of cardiac differentiation using this method resulted in beating cardiomyocytes at Day 9 of culture. Three weeks post initial contraction, cardiomyocytes were labelled with SIRPA, intracellular MLC2A and MLC2V antibodies using MARIS [19, 20], followed by FACS to isolate MLC2A+ and MLC2V+ cardiomyocytes. Figure 1B showed the FACS plots of the gating strategy for isolation of MLC2A+ and MLC2V+ cardiomyocytes. RNA sequencing was then conducted to examine the gene expression profile of MLC2A+ and MLC2V+ cardiomyocytes. The results revealed a significant difference in the gene expression between the two subtypes of CMs derived from BJ line, with a total of 2865 genes showing differential expression. Of these, 1349 and 1516 genes were significantly up- and down-regulated, respectively, in the BJ MLC2V+ samples compared to BJ MLC2A+ samples (Additional file 1: Table S1). Additionally, a comparison of differentially expressed genes was also performed between ES03 MLC2V+ and BJ MLC2A+ samples, revealing that 1904 and 2811 genes were significantly up- and down-regulated, respectively (Additional file 2: Table S2). The top 500 genes across the samples were used to conduct hierarchical clustering, and the resulting dendrogram (Fig. 1C) clearly demonstrated a distinct separation between MLC2V-sorted CMs samples and MLC2A-sorted CMs samples, regardless of the PSC lines that were used.

To identify potential surface marker candidates that play a role in ventricular specification, we focused on genes that were significantly up-regulated in MLC2V+ samples, as compared to MLC2A+ samples. To further refine the list of potential surface marker candidates, only genes that were up-regulated in both BJ and ES03 MLC2V+ samples were taken into consideration. By cross-referencing these commonly up-regulated genes in both BJ and ES03 MLC2V+ samples with our previous research findings on the list of membrane receptors expressed in hESCs [34] and GeneCards human gene database (<http://www.genecards.org>), we discovered 30 putative surface markers for ventricular-specific cardiomyocytes (Additional file 3: Table S3), as presented in Fig. 1D. Among these candidates, JAK2 and CD200 were selected for further investigation.

SIRPA+/JAK2+ and SIRPA+/CD200+ populations were enriched for ventricular-like cardiomyocytes

To assess the effectiveness of the putative cell surface markers in purifying ventricular-specific cardiomyocytes, FACS sorting was employed to isolate different subsets of cardiomyocytes expressing SIRPA alone, SIRPA+/JAK2+, SIRPA+/JAK2-, SIRPA+/CD200+ and SIRPA+/CD200-. Analysis via immunofluorescent staining of SIRPA+ only cardiomyocytes indicated the presence of a mixed population of MLC2V- and MLC2A-expressing cells (Additional file 4: Fig. S1). Specifically, for BJ-derived CMs, approximately 48 \pm 12% and 52 \pm 10% of SIRPA+ CMs expressed MLC2V and MLC2A, respectively. Similar findings were obtained for H7-derived CMs, where 43 \pm 6% and 57 \pm 6% of SIRPA+ cells were MLC2V+ and MLC2A+, respectively. These results are consistent with previous reports where sorting with SIRPA alone did not result in specific cardiac subtype enrichment [35].

On the contrary, we demonstrated that purification based on SIRPA/JAK2 expression led to an enrichment of ventricular-like CMs, as evidenced by a higher percentage of MLC2V-expressing cells (89 \pm 4% and 82 \pm 7%) in the SIRPA+/JAK2+ cell population compared to the SIRPA+/JAK2- population (56 \pm 5% and 53 \pm 5% of MLC2V+ cells) in both BJ and H7 cell lines, respectively (Fig. 2B). Similarly, isolation of SIRPA+/CD200+ CMs resulted in up to 70 \pm 5% (BJ) and 74 \pm 5% (H7) purity of ventricular-like CMs (Fig. 3B).

Consistent findings were observed between western blot results and immunofluorescent staining. We noted an increased expression of the ventricular-specific MLC2V protein and decreased expression of MLC2A

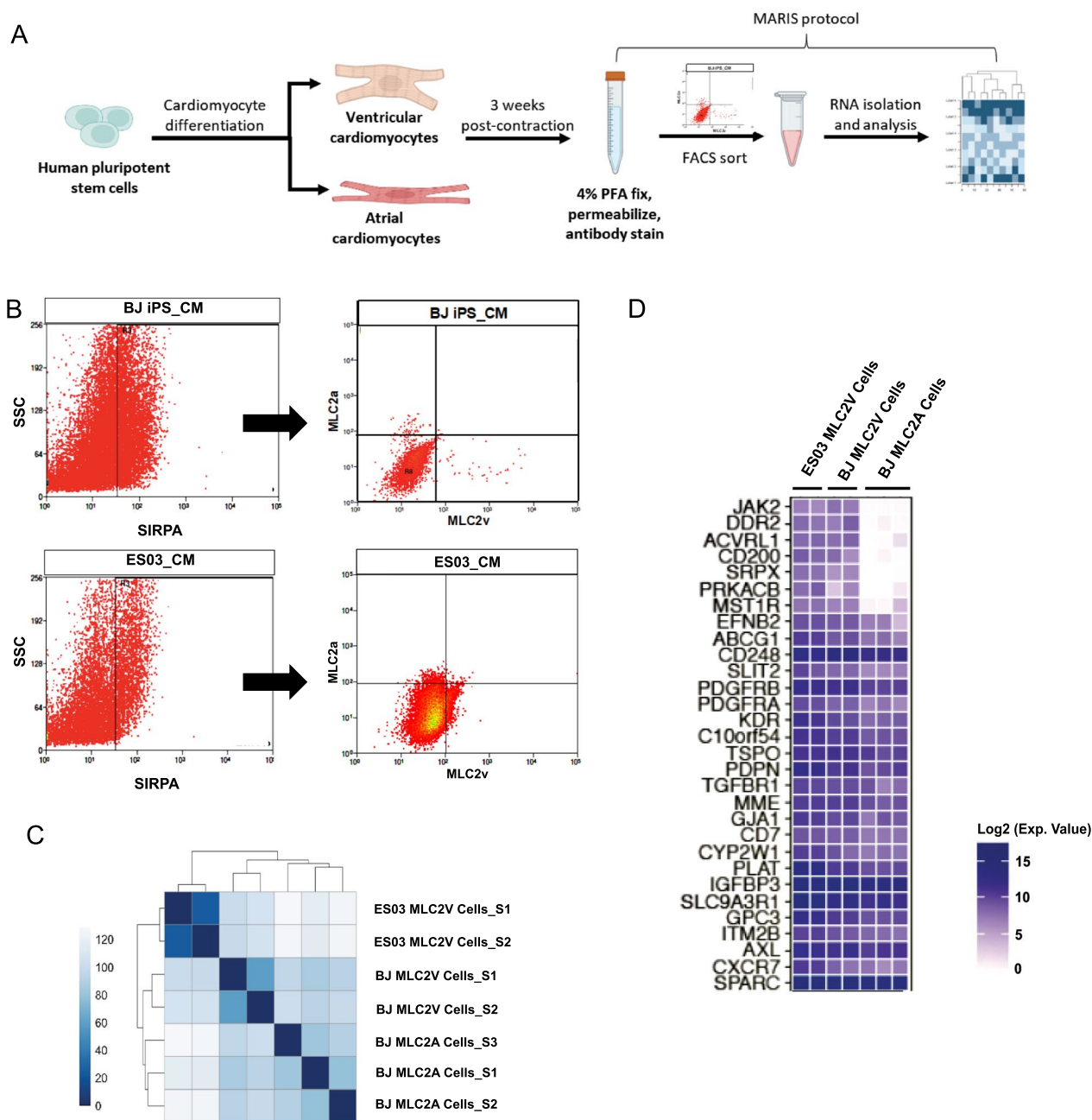


Fig. 1 JAK2 and CD200 as potential surface markers for ventricular-specific cardiomyocytes. **A** Schematic diagram illustrating the protocol used to identify putative surface markers for ventricular-specific CMs. Created with BioRender.com. **B** Gating strategy for isolation of MLC2A+ and MLC2V+ cardiomyocytes derived from BJ and ES03 lines by FACS. **C** Hierarchical clustering analysis of the top 500 differentially expressed genes revealed a distinct separation between MLC2V+ and MLC2A+ samples. **D** Heatmap showing the list of putative surface marker genes for ventricular-specific cardiomyocytes identified through RNA sequencing analysis

proteins in the SIRPA+/JAK2+ (Fig. 2C, Additional file 5: Fig. S2 and Additional file 6: Fig. S3) or SIRPA+/CD200+ (Fig. 3C, Additional file 6: Fig. S3 and Additional file 7: Fig. S4) sorted population in both cell lines.

SIRPA +/JAK2 + and SIRPA +/CD200 + sorted cardiomyocytes displayed electrophysiological properties similar to the ventricular-like cardiomyocytes

Atrial and ventricular cardiomyocytes exhibit distinct calcium transient profiles [36]. To characterize the electrophysiological properties of surface markers-sorted

cardiomyocytes, we utilized fluo-4 AM, a green-fluorescent calcium indicator, to measure the cellular calcium transient at the single cell level. We analysed various parameters, including beat-to-beat duration, depolarization and repolarization phase duration (Fig. 4A and Additional file 8: Fig. S5). Through calcium imaging analysis, we observed distinct calcium transient morphology in both the positive- and negative-sorted populations, regardless of the surface marker used (Fig. 4B). Notably, the majority of CMs sorted positive for JAK2 and CD200 surface markers displayed a significantly slower depolarization time (time to peak) compared to SIRPA+/JAK2- and SIRPA+/CD200- populations (Fig. 4C). Additionally, SIRPA+/JAK2+ and SIRPA+/CD200+ CMs exhibited a significantly longer repolarization duration at 30%, 60% and 90%, indicating ventricular-like electrophysiological properties (Fig. 4D). Conversely, SIRPA+/JAK2- and SIRPA+/CD200- populations contained a considerable number of CMs with a significantly shorter repolarization time, indicative of human atrial-like electrophysiology. Furthermore, when comparing beat-to-beat durations, we observed pronounced differences in beating frequency. Specifically, SIRPA+/JAK2+ and SIRPA+/CD200+ populations exhibited slower beating rates compared to their respective negative populations, resembling the properties of CMs from the human ventricle (Fig. 4E).

SIRPA+/JAK2+ and SIRPA+/CD200+ CMs did not respond to vernakalant treatment, an atrial-selective anti-arrhythmic agent

Finally, we performed functional validation on the surface markers-sorted cardiomyocytes by investigating their response towards treatment with vernakalant. Vernakalant is an anti-arrhythmic agent that selectively targets atrial CMs by blocking the potassium channels and prolonging the repolarization phase in these cells [37]. Given this mechanism of action, it is therefore reasonable to infer that vernakalant treatment would primarily affect the population containing a significant amount of atrial CMs, rather than ventricular CMs.

In this study, we treated the surface marker-sorted CMs with 10 μ M vernakalant and assessed their calcium

transient profile at three different stages, namely the pre-treatment, post-treatment and withdrawal stages of vernakalant (see Fig. 5A) [38]. We observed a distinct change in the calcium transient profile of the CMs from the SIRPA+/JAK2- and SIRPA+/CD200- populations upon treatment with vernakalant. Specifically, the repolarization duration of these CMs at 30%, 60% and 90% was significantly prolonged in both BJ and H7 cell lines (right panels in Fig. 5B and 5C). This effect was reversed upon removal of vernakalant through a repeated washing procedure. In contrast, CMs from the SIRPA+/JAK2+ and SIRPA+/CD200+ populations exhibited minimal to no significant response to vernakalant, indicating an enrichment of ventricular-like CMs in these populations (left panels in Fig. 5B, C).

Although we observed a slight increase in the repolarization duration at 30% and 60% in BJ SIRPA+/JAK2+ cardiomyocytes following vernakalant treatment, we considered this effect to be negligible as the extent of elongation was very minor when compared to the significant changes observed in BJ SIRPA+/JAK2- cells.

Discussion

The generation and purification of cardiomyocyte sub-population are critical for precise modelling of cardiac diseases, drug screening and regenerative medicine development due to their distinct phenotypic and functional characteristics. Therefore, identifying surface markers for cardiomyocyte subtype that facilitate live cell sorting of homogenous population of cardiomyocytes is of utmost importance for successful translation of cardiovascular research and therapeutic applications.

In the present study, we identified CD200 and JAK2 as potential candidate surface markers for purifying ventricular CMs. CD200 is a cell surface glycoprotein belonging to the immunoglobulin superfamily [39], while JAK2 is a member of the Janus kinase (JAKs) family with several reports suggested different localization, including cytoplasm [40], cell surface or plasma membrane [41, 42]. While our study reported CD200 to be a potential cell surface marker for ventricular CM, an earlier study by Veevers et al. reported that CD200 is negatively associated with ventricular CMs [43]. In that study, the authors

(See figure on next page.)

Fig. 2 SIRPA+/JAK2+ population shows enrichment of ventricular CMs. **A** Representative FACS plots of CMs sorted using SIRPA and JAK2 antibodies. Unstained CMs served as negative control. **B** Representative images of SIRPA+/JAK2+ (top panel) and SIRPA+/JAK2- (bottom panel) CMs co-stained with MLC2V and MLC2A antibodies. Nucleus was stained with DAPI. The percentage of MLC2V+ and MLC2A+ CMs in the respective populations was quantified and expressed as mean \pm SD. * $P < 0.05$, ** $P < 0.01$, *** $P < 0.001$, **** $P < 0.0001$ (t test). Data were collected from duplicate experiments. Scale bar = 100 μ m. **C** Western blot analysis of MLC2A and MLC2V expression in SIRPA+/JAK2+ and SIRPA+/JAK2- populations, normalized to GAPDH expression. Full-length blots are presented in Additional file 5: Fig. S2 (for BJ SIRPA/JAK2 sorted samples) and Additional file 6: Fig. S3 (for H7 SIRPA/JAK2 sorted samples)

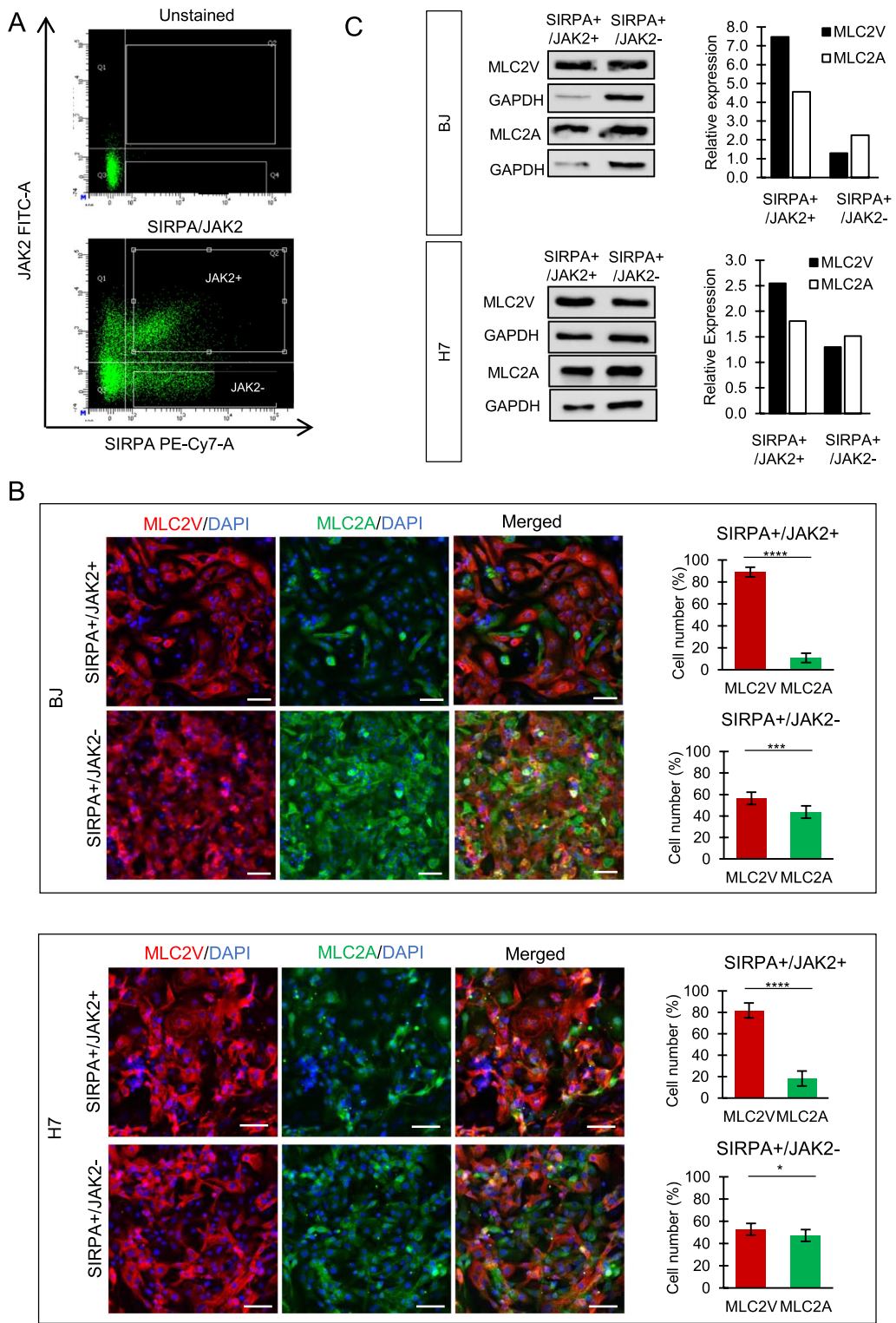


Fig. 2 (See legend on previous page.)

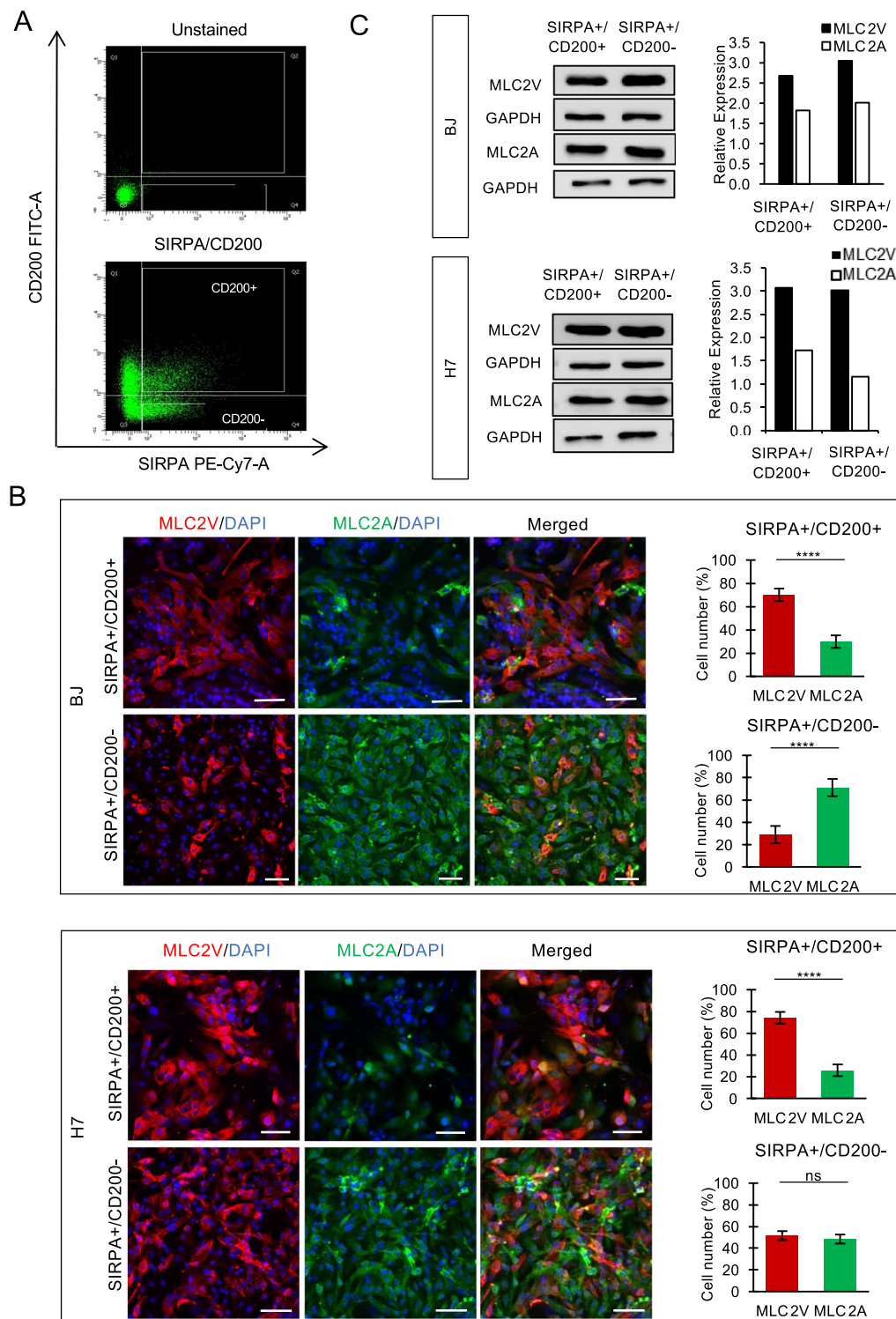


Fig. 3 SIRPA+/CD200+ population shows enrichment of ventricular CMs. **A** Representative FACS plots of CMs sorted using SIRPA and CD200 antibodies. Unstained CMs served as negative control. **B** Representative images of SIRPA+/CD200+ (top panel) and SIRPA+/CD200- (bottom panel) CMs co-stained with MLC2V and MLC2A antibodies. Nucleus were stained with DAPI. The percentage of MLC2V+ and MLC2A+ CMs in the respective populations was quantified and expressed as mean \pm SD. * $P < 0.05$, ** $P < 0.01$, *** $P < 0.001$, **** $P < 0.0001$ (t test). Data were collected from duplicate experiments. Scale bar = 100 μ m. **C** Western blot analysis of MLC2A and MLC2V expression in SIRPA+/CD200+ and SIRPA+/CD200- populations, normalized to GAPDH expression. Full-length blots are presented in Additional file 6: Fig. S3 (for BJ SIRPA/CD200 sorted samples) and Additional file 7: Fig. S4 (for H7 SIRPA/CD200 sorted samples)

used a panel of 242 known anti-human monoclonal antibodies to screen through a hPSC line harbouring GFP reporter driven by MYL2 promoter to show that CD77+/CD200– are cell surface markers for ventricular CMs. While they showed that 65% of the CD77+/CD200– population expressed MYL2-GFP, suggesting that they are ventricular CMs, it was subsequently reported that there is little to no expression of CD77 detected in CMs derived from two independent wildtype iPSC lines, hampering its application in all hPSC lines [43].

In the current study, we have employed a different approach that utilized MARIS, coupled with RNA sequencing analysis on MLC2A- and MLC2V-expressing cardiomyocytes to identify potential surface markers that can be used to isolate specific cardiomyocyte sub-populations. This method enables profiling of rare cell types that are difficult to isolate using traditional sorting approaches while maintaining cellular integrity and improving the accuracy of gene expression analysis. Importantly, isolation of CMs through the use of cell surface markers eliminates the need for genetic modification, which in turn minimizes safety concerns such as the inadvertent activation of oncogenes or the introduction of novel allergenic or immunogenic elements. This is particularly relevant for therapeutic applications such as cell transplantation, where safety is of utmost importance.

While we identified CD200 as one of the potential ventricular cell surface markers, we achieved a marginal increase in the enrichment of ventricular-like CMs (70%-75%) when sorting together with SIRPA antibody (SIRPA+/CD200+) as compared to the unsorted (SIRPA+ only) population (up to 43%-48%). In contrast, purification based on SIRPA+/JAK2+ expression led to a significant enrichment of ventricular-like CMs (~90%). To further validate these surface markers, we utilized MYL2-TdTomato reporter system generated from H7 embryonic stem cell (ESC) line (H7-MYL2-TdTomato). Remarkably, among the TdTomato-positive cardiomyocytes, 71.25% exhibited co-expression of SIRPA and JAK2, while 48.5% displayed co-expression of SIRPA and CD200 (Additional file 9: Fig. S6). This additional finding further supports our assertion regarding the potential of SIRPA/JAK2 cell surface markers in facilitating the isolation of ventricular cardiomyocytes. Interestingly, while CD200 and JAK2 expressions are not mutually exclusive

in the ventricular cardiomyocyte sub-population, the utility of using both CD200 and JAK2 did not produce a synergistic effect in enhancing the purity of ventricular cardiomyocytes (data not shown). At the molecular level, RNA sequencing revealed that gene expression profiles of SIRPA+/JAK2+ cardiomyocytes closely resembled those of H7-MYL2-TdTomato+ cardiomyocytes. In addition, SIRPA+/JAK2+ CMs exhibited high expression levels of ventricular-associated genes previously reported [44–46], including MYL2, HEY2, IRX4 and DLK1, comparable to ventricular CMs generated from reporter line and adult human ventricle samples (Additional file 10: Fig. S7).

Conclusion

Taken together, our study has identified CD200 and JAK2 as potential surface markers for ventricular-like cardiomyocytes, with SIRPA+/JAK2+ achieving a higher purity in isolating ventricular subtype. The results illustrated JAK2 as a novel surface marker for the purification of stem cells-derived ventricular CM. By enhancing the purity of ventricular CMs, it could potentially improve drug screening processes or transplantation outcome by mitigating the risk of arrhythmic phenotype.

(See figure on next page.)

Fig. 4 Electrophysiological characterization of SIRPA+ CMs sorted with JAK2 or CD200 surface markers. **A** Workflow of the calcium imaging analysis for surface markers-sorted CMs. Created with BioRender.com. **B** Representative kymographs and the corresponding calcium transient profiles for CMs sorted with JAK2 and CD200 surface markers. **C, D, E** Dot plot showing mean of **C** calcium depolarization duration, **D** calcium repolarization duration at 30%, 60% and 90%, and **E** beat-to-beat duration in SIRPA/JAK2 and SIRPA/CD200 sorted cardiomyocytes. *P < 0.05, **P < 0.01, ***P < 0.001, ****P < 0.0001 (t test)

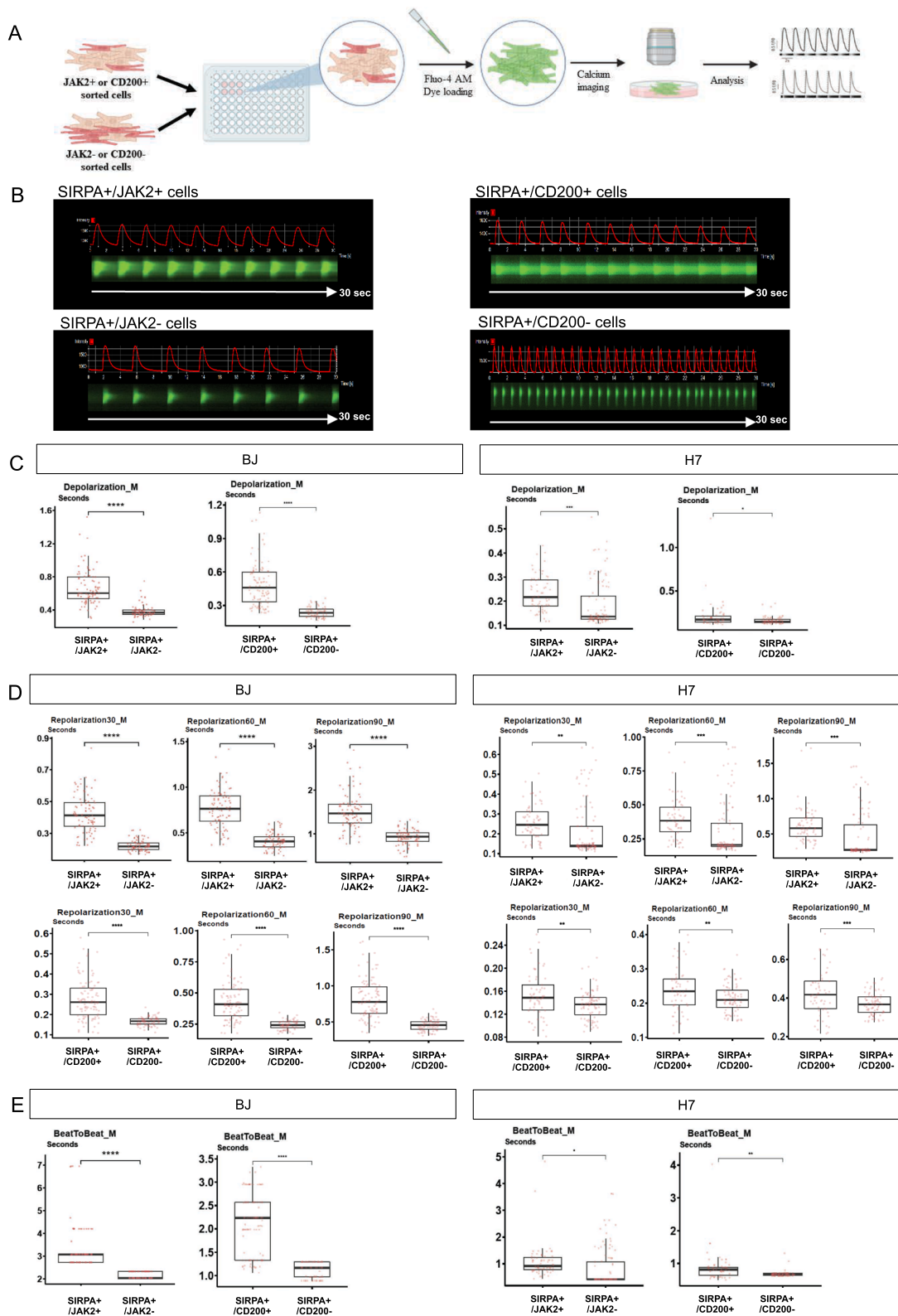


Fig. 4 (See legend on previous page.)

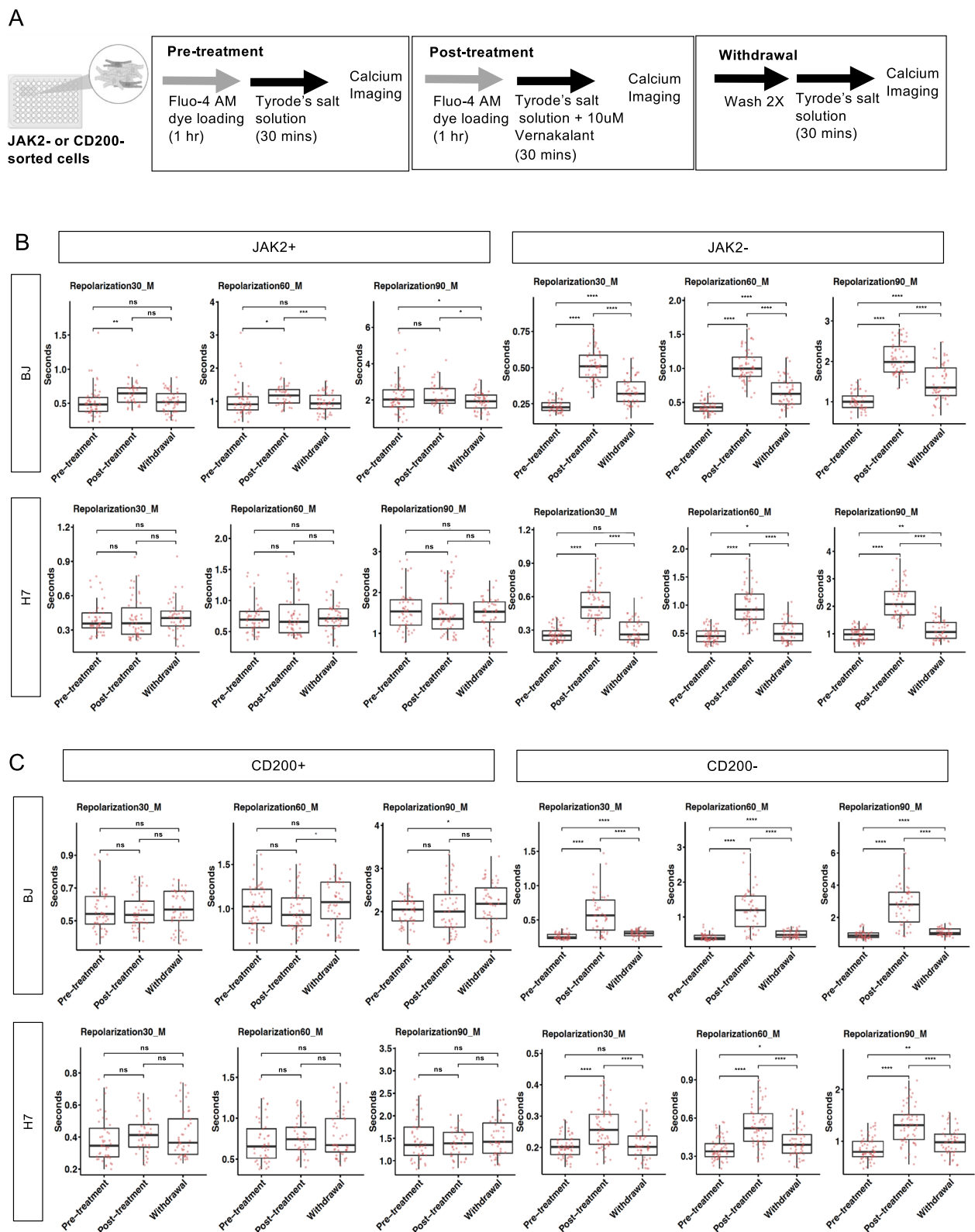


Fig. 5 Electrophysiological characterization of SIRPA +CMs sorted with JAK2 or CD200 surface markers treated with vernakalant. **A** Schematic showing calcium imaging workflow for the evaluation of the effects of vernakalant on CMs sorted with surface markers. Created with BioRender.com. **B, C** Effect of 10 μ m vernakalant treatment on the mean of repolarization duration (at 30%, 60% and 90%) in **B** SIRPA/JAK2 and **C** SIRPA/CD200 sorted cardiomyocytes. *P < 0.05, **P < 0.01, ***P < 0.001, ****P < 0.0001 (t test)

Abbreviations

hPSC	Human pluripotent stem cell
CMs	Cardiomyocytes
MLC2A	Myosin light chain 2A
MLC2V	Myosin light chain 2V
JAK2	Janus kinase 2
hESCs	Human embryonic stem cells
hiPSCs	Human-induced pluripotent stem cells
CVDs	Cardiovascular diseases
COUP-TFII	Chick ovalbumin upstream promoter transcription factor II
MARIS	Method for analysing RNA following intracellular sorting
GFAM	Glucose-depleted culture medium supplemented with fatty acid
GSK-3	Glycogen synthase kinase 3
BSA	Bovine serum albumin
PBS	Phosphate-buffered saline
DPBS	Dulbecco's phosphate-buffered saline
FACS	Florescence activated cell sorting
FBS	Foetal bovine serum
RT	Room temperature
SD	Standard deviation
SIRPA	Signal regulatory protein alpha

Supplementary Information

The online version contains supplementary material available at <https://doi.org/10.1186/s13287-023-03610-2>.

Additional file 1: Table S1. List of differentially expressed genes between BJ MLC2V+ and BJ MLC2A+ cardiomyocytes identified by RNA-Seq analysis.

Additional file 2: Table S2. List of differentially expressed genes between ES03 MLC2V+ and BJ MLC2A+ cardiomyocytes identified by RNA-Seq analysis.

Additional file 3: Table S3. List of putative surface markers for isolation of ventricular-specific cardiomyocytes.

Additional file 4: Figure S1. Representative images of SIRPA+ only CMs co-stained with MLC2V and MLC2A antibodies, followed by quantification of the percentage of MLC2V+ and MLC2A+ CMs. All values are expressed as mean \pm SD. * $P < 0.05$, ** $P < 0.01$, *** $P < 0.001$, **** $P < 0.0001$ (t test). Data were collected from duplicate experiments.

Additional file 5: Figure S2. Full-length blots of MLC2V (left blot), MLC2A (right blot) and the respective GAPDH expressions in SIRPA+/JAK2+ and SIRPA+/JAK2- populations for BJ cell line. Red boxes indicate the cropped blots shown in Fig. 2C.

Additional file 6: Figure S3. Full-length blots of MLC2V (left blot), MLC2A (right blot) and the respective GAPDH expressions in SIRPA+/JAK2+, SIRPA+/JAK2-, SIRPA+/CD200+ and SIRPA+/CD200- populations. Red boxes indicate the cropped blots shown in Fig. 2C (H7 SIRPA/JAK2) and Fig. 3C (BJ SIRPA/CD200).

Additional file 7: Figure S4. Full-length blots of MLC2V (left blot), MLC2A (right blot) and the respective GAPDH expressions in SIRPA+/CD200+ and SIRPA+/CD200- populations for H7 cell line. Red boxes indicate the cropped blots shown in Fig. 3C.

Additional file 8: Figure S5. Schematic showing calcium transient profile derived per single cardiomyocyte contraction rhythm. The diagram illustrates the various parameters that were measured in each cardiomyocyte contraction cycle, including calcium transient amplitude, depolarisation and repolarization phase duration.

Additional file 9: Figure S6. Validation of surface markers-sorted CMs using MYL2 reporter line. **A** Representative FACS plots showing the co-staining of SIRPA/JAK2 or SIRPA/CD200 antibodies in H7-MYL2-TdTomato-derived CMs. Unstained CMs derived from H7 wild type were used as a negative control. **B** Quantification of the percentage of SIRPA+/JAK2+ and SIRPA+/CD200+ cells within the TdTomato+ population, presented as mean \pm SD. The data were obtained from duplicate experiments.

Additional file 10: Figure S7. RNA sequencing analysis comparing gene expression profiles across different samples. **A** Heatmap illustrating the top 100 of atrial and ventricular genes in human adult atria and ventricle tissue. Heatmap depicting the expression of top 100 ventricular genes in SIRPA+/JAK2+ cardiomyocytes, in comparison with **B** H7-MYL2-TdTomato+ cardiomyocytes and **C** samples obtained from the adult human atria and ventricle of the heart. **D** Assessment of ventricular- and atrial-specific gene expressions across diverse sample sets.

Acknowledgements

The authors would like to thank the SBIC-Nikon Imaging Centre at Biopolis and their supporting staff for the microscopy data and images that were acquired in this study.

Author contributions

L.C.L. designed and performed most of the experiments, analysed data and wrote the manuscript. B.M.P. assisted in experimental design, experimental work, data analysis, review and edit the manuscript. O.A., J.K.S.P., L.Y.B. and H.H.Y. performed gene expression profiling. B.X.H. and C.Y.Y.L. assisted in experimental work. B.S.S. conceptualized and supervised the study, performed MARIS experiment, review and edit the manuscript.

Funding

This work is partially supported by the Agency for Science, Technology and Research (Singapore) and by a grant to B.S.S. (ETPL/18-GAP028-R20H). This work is also supported in part by ThermoFisher, USA. L.C.L. is partly supported by A*STAR Grant No. C210812006. The funding body played no role in the design of the study and collection, analysis and interpretation of data and in writing the manuscript.

Availability of data and materials

The data discussed in this publication have been deposited in NCBI's Gene Expression Omnibus and are accessible through GEO Series accession number GSE231913 (<https://www.ncbi.nlm.nih.gov/geo/query/acc.cgi?acc=GSE231913>).

Declarations

Ethics approval and consent to participate

Not applicable.

Consent for publication

Not applicable.

Competing interests

The authors declare no competing interests.

Author details

¹Institute of Molecular and Cell Biology (IMCB), Agency for Science, Technology and Research (A*STAR), 61 Biopolis Drive, Proteos, Singapore 138673, Republic of Singapore. ²Cancer Science Institute of Singapore, National University of Singapore, Singapore 117599, Republic of Singapore. ³Department of Biological Sciences, National University of Singapore, Singapore 117543, Republic of Singapore.

Received: 26 April 2023 Accepted: 7 December 2023

Published online: 13 December 2023

References

- Thomson JA, Itskovitz-Eldor J, Shapiro SS, Waknitz MA, Swiergiel JJ, Marshall VS, et al. Embryonic stem cell lines derived from human blastocysts. *Science*. 1998;282(5391):1145–7.
- Takahashi K, Tanabe K, Ohnuki M, Narita M, Ichisaka T, Tomoda K, et al. Induction of pluripotent stem cells from adult human fibroblasts by defined factors. *Cell*. 2007;131(5):861–72.

3. Carvajal-Vergara X, Sevilla A, D'Souza SL, Ang YS, Schaniel C, Lee DF, et al. Patient-specific induced pluripotent stem-cell-derived models of LEOP-ARD syndrome. *Nature*. 2010;465(7299):808–12.
4. Itzhaki I, Maizels L, Huber I, Zwi-Dantsis L, Caspi O, Winterstern A, et al. Modelling the long QT syndrome with induced pluripotent stem cells. *Nature*. 2011;471(7337):225–9.
5. Hinson JT, Chopra A, Nafissi N, Polacheck WJ, Benson CC, Swist S, et al. HEART DISEASE Titin mutations in iPS cells define sarcomere insufficiency as a cause of dilated cardiomyopathy. *Science*. 2015;349(6251):982–6.
6. Cao F, Wagner RA, Wilson KD, Xie X, Fu JD, Drukker M, et al. Transcriptional and functional profiling of human embryonic stem cell-derived cardiomyocytes. *PLoS ONE*. 2008;3(10): e3474.
7. He JQ, Ma Y, Lee Y, Thomson JA, Kamp TJ. Human embryonic stem cells develop into multiple types of cardiac myocytes: action potential characterization. *Circ Res*. 2003;93(1):32–9.
8. Zhang J, Wilson GF, Soerens AG, Koonce CH, Yu J, Palecek SP, et al. Functional cardiomyocytes derived from human induced pluripotent stem cells. *Circ Res*. 2009;104(4):e30–41.
9. Ma J, Guo L, Fiene SJ, Anson BD, Thomson JA, Kamp TJ, et al. High purity human-induced pluripotent stem cell-derived cardiomyocytes: electrophysiological properties of action potentials and ionic currents. *Am J Physiol Heart Circ Physiol*. 2011;301(5):H2006–17.
10. Shiba Y, Gomibuchi T, Seto T, Wada Y, Ichimura H, Tanaka Y, et al. Allogeneic transplantation of iPSC cell-derived cardiomyocytes regenerates primate hearts. *Nature*. 2016;538(7625):388–91.
11. Zhang Q, Jiang J, Han P, Yuan Q, Zhang J, Zhang X, et al. Direct differentiation of atrial and ventricular myocytes from human embryonic stem cells by alternating retinoid signals. *Cell Res*. 2011;21(4):579–87.
12. Lee JH, Protze SI, Laksman Z, Backx PH, Keller GM. Human pluripotent stem cell-derived atrial and ventricular cardiomyocytes develop from distinct mesoderm populations. *Cell Stem Cell*. 2017;21(2):179–94.
13. Karakikes I, Senyei GD, Hansen J, Kong CW, Azeloglu EU, Stillitano F, et al. Small molecule-mediated directed differentiation of human embryonic stem cells toward ventricular cardiomyocytes. *Stem Cells Transl Med*. 2014;3(1):18–31.
14. Li B, Yang H, Wang X, Zhan Y, Sheng W, Cai H, et al. Engineering human ventricular heart muscles based on a highly efficient system for purification of human pluripotent stem cell-derived ventricular cardiomyocytes. *Stem Cell Res Ther*. 2017;8(1):202.
15. Yamauchi K, Li J, Morikawa K, Liu L, Shirayoshi Y, Nakatsuji N, et al. Isolation and characterization of ventricular-like cells derived from NKX2-5(eGFP/w) and MLC2v(mCherry/w) double knock-in human pluripotent stem cells. *Biochem Biophys Res Commun*. 2018;495(1):1278–84.
16. Schwach V, Verkerk AO, Mol M, Monshouwer-Kloots JJ, Devalla HD, Orlova VV, et al. A COUP-TFII human embryonic stem cell reporter line to identify and select atrial cardiomyocytes. *Stem Cell Rep*. 2017;9(6):1765–79.
17. Lian X, Zhang J, Azarin SM, Zhu K, Hazeltine LB, Bao X, et al. Directed cardiomyocyte differentiation from human pluripotent stem cells by modulating Wnt/beta-catenin signaling under fully defined conditions. *Nat Protoc*. 2013;8(1):162–75.
18. Correia C, Koshkin A, Duarte P, Hu D, Teixeira A, Domian I, et al. Distinct carbon sources affect structural and functional maturation of cardiomyocytes derived from human pluripotent stem cells. *Sci Rep*. 2017;7(1):8590.
19. Ng SY, Soh BS, Rodriguez-Muela N, Hendrickson DG, Price F, Rinn JL, et al. Genome-wide RNA-Seq of human motor neurons implicates selective ER stress activation in spinal muscular atrophy. *Cell Stem Cell*. 2015;17(5):569–84.
20. Hrvatin S, Deng F, O'Donnell CW, Gifford DK, Melton DA. MARIS: method for analyzing RNA following intracellular sorting. *PLoS ONE*. 2014;9(3): e89459.
21. An Q, Tan K, Li Y, Li J, Wu C, Zhang B, et al. CSI NGS portal: an online platform for automated NGS data analysis and sharing. Preprints. 2019;2019100146.
22. Bolger AM, Lohse M, Usadel B. Trimmomatic: a flexible trimmer for Illumina sequence data. *Bioinformatics*. 2014;30(15):2114–20.
23. Dobin A, Davis CA, Schlesinger F, Drenkow J, Zaleski C, Jha S, et al. STAR: ultrafast universal RNA-seq aligner. *Bioinformatics*. 2013;29(1):15–21.
24. Anders S, Pyl PT, Huber W. HTSeq—a Python framework to work with high-throughput sequencing data. *Bioinformatics*. 2015;31(2):166–9.
25. Collado-Torres L, Jaffe AE, Leek JT. regionReport: interactive reports for region-level and feature-level genomic analyses. *F1000Res*. 2015;4:105.
26. Love MI, Huber W, Anders S. Moderated estimation of fold change and dispersion for RNA-seq data with DESeq2. *Genome Biol*. 2014;15(12):550.
27. Chen S, Zhou Y, Chen Y, Gu J. fastp: an ultra-fast all-in-one FASTQ preprocessor. *Bioinformatics*. 2018;34(17):i884–90.
28. Chen S. Ultrafast one-pass FASTQ data preprocessing, quality control, and deduplication using fastp. *iMeta*. 2023;2(2).
29. Wang L, Wang S, Li W. RSEQC: quality control of RNA-seq experiments. *Bioinformatics*. 2012;28(16):2184–5.
30. Love MI, Anders S, Kim V, Huber W. RNA-Seq workflow: gene-level exploratory analysis and differential expression. *F1000Res*. 2015;4:1070.
31. Pang JKS, Chia S, Zhang J, Szyniarowski P, Stewart C, Yang H, et al. Characterizing arrhythmia using machine learning analysis of Ca(2+) cycling in human cardiomyocytes. *Stem Cell Rep*. 2022;17(8):1810–23.
32. O'Brien TX, Lee KJ, Chien KR. Positional specification of ventricular myosin light chain 2 expression in the primitive murine heart tube. *Proc Natl Acad Sci U S A*. 1993;90(11):5157–61.
33. Kubalak SW, Miller-Hance WC, O'Brien TX, Dyson E, Chien KR. Chamber specification of atrial myosin light chain-2 expression precedes septation during murine cardiogenesis. *J Biol Chem*. 1994;269(24):16961–70.
34. Soh BS, Song CM, Vallier L, Li P, Choong C, Yeo BH, et al. Pleiotrophin enhances clonal growth and long-term expansion of human embryonic stem cells. *Stem Cells*. 2007;25(12):3029–37.
35. Boheler KR, Poon EN. Cell surface markers for immunophenotyping human pluripotent stem cell-derived cardiomyocytes. *Pflugers Arch*. 2021;473(7):1023–39.
36. Cyganek L, Tiburcy M, Sekeres K, Gerstenberg K, Bohnenberger H, Lenz C, et al. Deep phenotyping of human induced pluripotent stem cell-derived atrial and ventricular cardiomyocytes. *JCI Insight*. 2018;3(12).
37. Wettwer E, Christ T, Endig S, Rozmaritsa N, Matschke K, Lynch JJ, et al. The new antiarrhythmic drug vernakalant: ex vivo study of human atrial tissue from sinus rhythm and chronic atrial fibrillation. *Cardiovasc Res*. 2013;98(1):145–54.
38. Goldfracht I, Protze S, Shiti A, Setter N, Gruber A, Shaheen N, et al. Generating ring-shaped engineered heart tissues from ventricular and atrial human pluripotent stem cell-derived cardiomyocytes. *Nat Commun*. 2020;11(1):75.
39. D'Arena G, De Feo V, Pietrantonio G, Seneca E, Mansueto G, Villani O, et al. CD200 and chronic lymphocytic leukemia: biological and clinical relevance. *Front Oncol*. 2020;10: 584427.
40. Lee S, Duhe RJ. Kinase activity and subcellular distribution of a chimeric green fluorescent protein-tagged Janus kinase 2. *J Biomed Sci*. 2006;13(6):773–86.
41. Behrmann I, Smyczek T, Heinrich PC, Schmitz-Van de Leur H, Komyod W, Giese B, et al. Janus kinase (Jak) subcellular localization revisited: the exclusive membrane localization of endogenous Janus kinase 1 by cytokine receptor interaction uncovers the Jak receptor complex to be equivalent to a receptor tyrosine kinase. *J Biol Chem*. 2004;279(34):35486–93.
42. Moulin S, Bouzinba-Segard H, Kelly PA, Finidori J. Subcellular trafficking of growth hormone receptor and Jak2 under ligand exposure. *Horm Metab Res*. 2003;35(7):396–401.
43. Veevers J, Farah EN, Corselli M, Witty AD, Palomares K, Vidal JG, et al. Cell-surface marker signature for enrichment of ventricular cardiomyocytes derived from human embryonic stem cells. *Stem Cell Rep*. 2018;11(3):828–41.
44. Ahn J, Wu H, Lee K. Integrative analysis revealing human heart-specific genes and consolidating heart-related phenotypes. *Front Genet*. 2020;11:777.
45. Piccini I, Rao J, Seebohm G, Greber B. Human pluripotent stem cell-derived cardiomyocytes: genome-wide expression profiling of long-term in vitro maturation in comparison to human heart tissue. *Genom Data*. 2015;4:69–72.
46. Churko JM, Garg P, Treutlein B, Venkatasubramanian M, Wu H, Lee J, et al. Defining human cardiac transcription factor hierarchies using integrated single-cell heterogeneity analysis. *Nat Commun*. 2018;9(1):4906.

Publisher's Note

Springer Nature remains neutral with regard to jurisdictional claims in published maps and institutional affiliations.